

Table S1. Summary of quality preprocessing in N192 and Ji853 mesocotyls under 3 cm sowing depth (CK), 20 cm sowing depth (DSS), 4.16×10^{-3} M 24-epibrassinolide (EBR) induction at 20 cm sowing depth (DSS+EBR) conditions by RNA-sequencing (RNA-Seq) data.

Sample	Raw Date Size (bp)	Clean Date Size (bp)	Clean Date Rate (%)	Total Reads	Q20 percentage (%)	Q30 percentage (%)	GC (%)	Mapped Reads	Mapping Rate (%)
N192(CK)	8041438907	7453056733	92.68	48818227	98.04	93.18	53.83	43377315	88.85
N192(DSS)	8385320530	7484737105	89.26	50458344	98.11	94.02	53.27	45568930	90.30
N192(DSS+EBR)	8135207165	7951351483	97.74	51659460	97.99	94.65	54.15	45444827	87.97
Ji853(CK)	7945756549	7198855434	90.61	49974282	98.09	94.52	53.98	44946869	89.94
Ji853(DSS)	8402899726	7881919943	93.85	53956450	98.14	94.64	54.36	48566200	90.01
Ji853(DSS+EBR)	8563313670	8272161005	96.59	53691625	98.2	94.27	54.22	48462060	90.26
Average	8245656091	7707013617	93.46	51426398	98.10	94.21	53.97	46061033	89.56

Table S2. The quantitative real-time (qRT-PCR) primer sequence.

Gene name	Gene ID	Forward primer (5' to 3')	Reverse primer (5' to 3')	Chromosome	Gene Position (bp)
Actin1	Zm00001d010159	CGATTGAGCATGGCATTGTCA	CCCACTAGCGTACAACGAA	8	102413768..102417536
PAL	Zm00001d003015	CTCATCCGATTCCCTCAATGC	GTCACGGTGGTGTGAGCAG	2	29467845..29470586
PAL	Zm00001d017276	CCGAGTACCGCCAACCCCT	CCAGTCGCTGCTTGCCCTT	5	191474509..191476978
C4H	Zm00001d016471	CAACTACGGCGACTTCATCC	CGTTGATGTTCTCGACGATGT	5	163692318..163694217
HCT	Zm00001d039947	CGCATGCAGCCTGAAGAGAT	AACGAGGTCCAGCGGAGAGA	3	20216146..20226938
C3'H	Zm00001d043174	GGGAAGCCGTTGGTTGTA	GGACGCACCGATCTTGATG	3	190625724..190628380
CCoAOMT	Zm00001d005998	GCAGCTCCTGATCGAGATT	GCGACCCATCTGGTCGTAG	2	194954891..194956278
CCR	Zm00001d032152	GCTGCTCGAGAACGGGATACAC	CGGGTCATCTGCTGCCAT	1	214573400..214579274
CAD	Zm00001d002346	TGCAGATCTCTGCCTTCTCTTT	GCGTTCATGGCCTCATTT	2	10649171..10653306
POD	Zm00001d009138	AAGGGCGTGAAGACCAA	TGCCGTGTAAGCTGAATAA	8	38826820..38828682
POD	Zm00001d053554	GCCCTCTCCGCTCAGACTT	TCAGCTGCTGTTGACCACCC	4	233852931..233854306
MYB	Zm00001d014029	AACTACCTCACCCGGACAT	GTGCCACACGTTCTTGATCTC	5	29347095..29349160
MYB	Zm00001d040621	GGCTGAGGCTGGTTTGT	GTTCGACCGGGCAAGTGA	3	54361983..54365788
MYB	Zm00001d008808	TAGGAAGTGCTCTAGCTGTGG	TGAAGCACCTCTTCATGGCTA	8	21238420..21240608
MYB	Zm00001d009435	GGGAAACAGGTGGTCGCA	GCGGCTTGCTCTGGTCGT	8	64426126..64427468
MYB	Zm00001d038288	GCTGTTCTGGAGGGGCTT	GTCGTGGATGCTTGTGCG	6	153438814..153440041
MYB	Zm00001d044117	AGTGGACGGCGAACAGAACAA	GTAGCGCCTGACCTCGTCCGCC	3	219796585..219798521
NAC	Zm00001d003626	TGTTTGCTGACGAGACGG	CGTCGAATCAAACACTCGGCATATC	2	50875214..50876868
NAC	Zm00001d006053	GCTTCAGGTTCCACCCGACT	CGTTCGCACGCCCTGTTGGTA	2	196582113..196584517
NAC	Zm00001d020982	TGGTGGTGGAGGGGGGAAGTCG	GACCGGTGAAGATTCTCTTATC	7	138832013..138836335
NAC	Zm00001d022517	CGCTGGACAGCCGCTTCTCCTG	CTGCTACTGCGCGGAAGAT	7	179273894..179275680
WRKY	Zm00001d008794	GGAGGAACAAGAACACGCA	CGAGGTGCTGGGGTCGTCGGT	8	20545292..20547558
WRKY	Zm00001d012505	ACGAGATCGCTACTACGGG	TCCAGGAACTCCATTACGGGATCAG	8	175577029..175578804
PEX14	Zm00001d011119	GCAGGTCAACAGCCAGAACATCA	AGCACCAAAACCAAGCAAGA	8	39412827..139416787
PXMP2	Zm00001d052410	CCATTTTCATTGGCGTCTTTA	CAAGGGCTACAAAATTAGCACC	4	189313573..189318465
MPV17	Zm00001d011761	CGGCTATGGGTATTCTCTT	GGTTTCATTTGCTCATTGTGGT	8	160949609..160951534
ACOX	Zm00001d045606	GTCATCCACAGTCCAACCTCAC	CACTACCGAACCTTCACCAAT	9	28565344..28570133
ACAA1	Zm00001d049882	AGGCAAGAGCAAGATCAGACC	ATCCACTCCAACAGCGGCA	4	50211783..50214016
CAT	Zm00001d027511	CGCACACCACAAACAACCACT	ACCGCTCTTGCCCTGCTG	1	7144389..7146665
SOD	Zm00001d031908	GCATAGCGAGGCAACCAT	CCCCCTTCCCAACCTCAT	1	206405747..206408926
MVK	Zm00001d054008	CTCCGCCTCCTTTCTCT	CAACACCTCCCAACCTCA	4	245047670..245055426

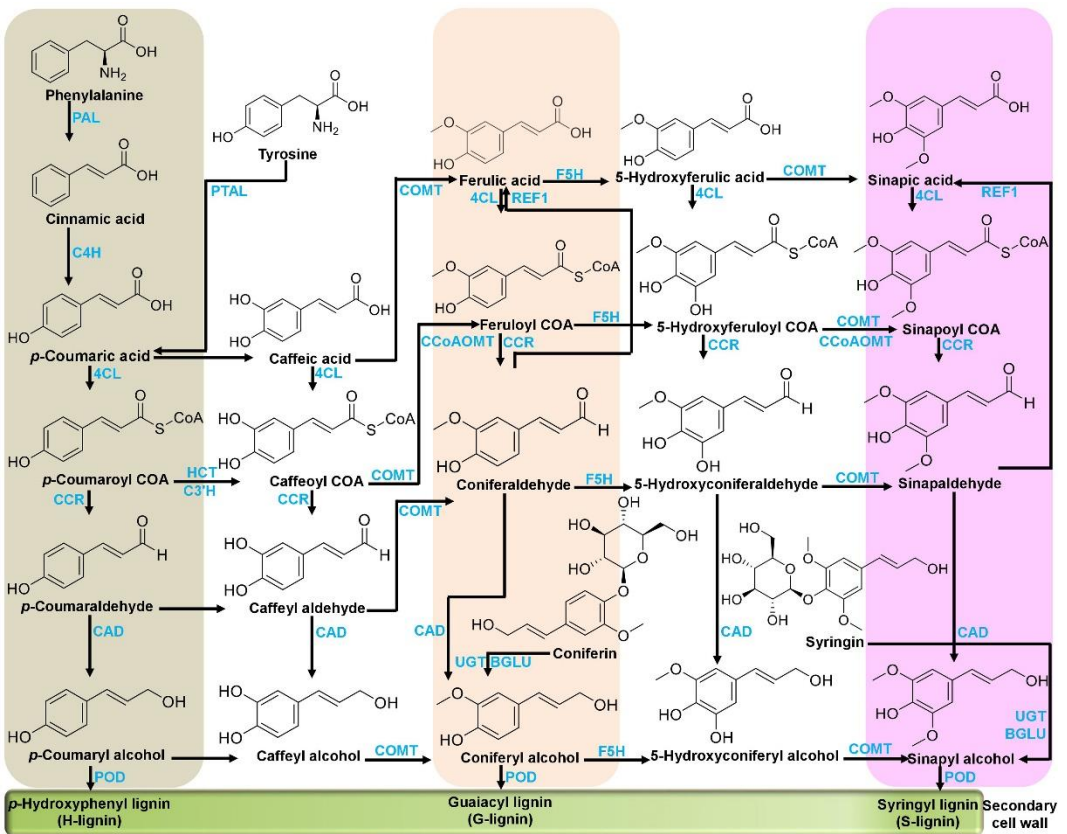


Figure S1. Phenylpropanoid pathway leading to lignin biosynthesis was showed in maize (phenylalanine ammonia-lyase [PAL], phenylalanine/tyrosine ammonia-lyase [PTAL], trans-cinnamate 4-monoxygenase [C4H], caffeoyl-CoA O-methyltransferase [CCoAOMT], caffeic acid O-methyltransferase [COMT], coniferyl-aldehyde dehydrogenase [REF1], 4-coumarate-CoA ligase [4CL], 5-O-(4-coumaroyl)-D-quinate 3'-monoxygenase [C3'H], ferulate-5-hydroxylase [F5H], shikimate O-hydroxycinnamoyltransferase [HCT], cinnamoyl-CoA reductase [CCR], cinnamyl-alcohol dehydrogenase [CAD], peroxidase [POD], laccase [LAC], beta-glucosidase [BGLU], and UDP-glucosyltransferase [UGT]).

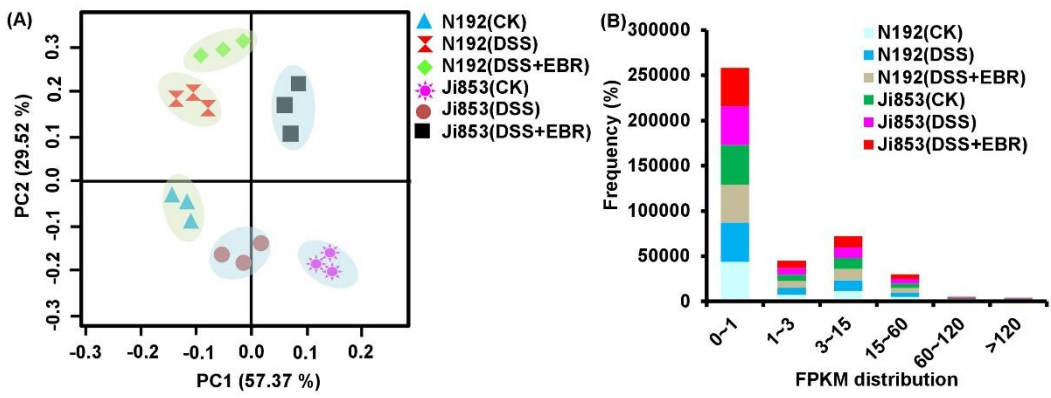


Figure S2. The principal component analysis (PCA) (A) and FPKM values distribution of corresponding genes (B) in N192 and Ji853 mesocotyls under 3 cm sowing depth (CK), 20 cm sowing depth (DSS), 4.16×10^{-3} M 24-epibrassinolide (EBR) induction at 20 cm sowing depth (DSS+EBR) conditions by RNA-sequencing (RNA-Seq) data.

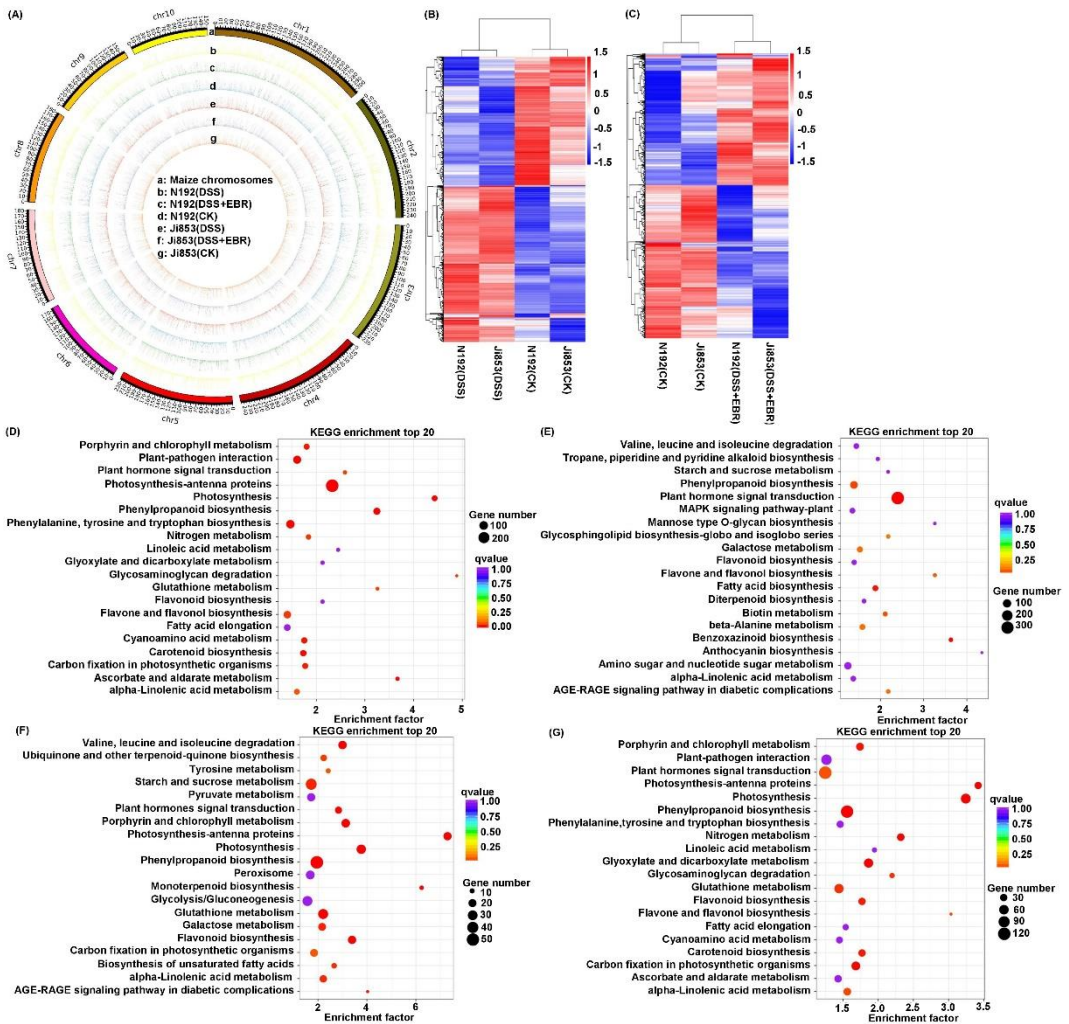


Figure S3. Distribution and expression profiles of differentially expressed genes (DEGs) and top 20 KEGG enrichment analysis in N192 and JI853 mesocotyls under CK, DSS, and DSS+EBR conditions. Distribution of DEGs in N192 and JI853 mesocotyl under three conditions (A). Based on the log₂ fold-change value of different comparisons, DEGs hierarchical clustering performed for three conditions to obtain six clusters (B and C). Top 20 KEGG pathways enriched by DEGs in N192 and JI853 mesocotyls under DSS conditions, respectively (D and E), and which under DSS+EBR conditions, respectively (F and G), respectively.

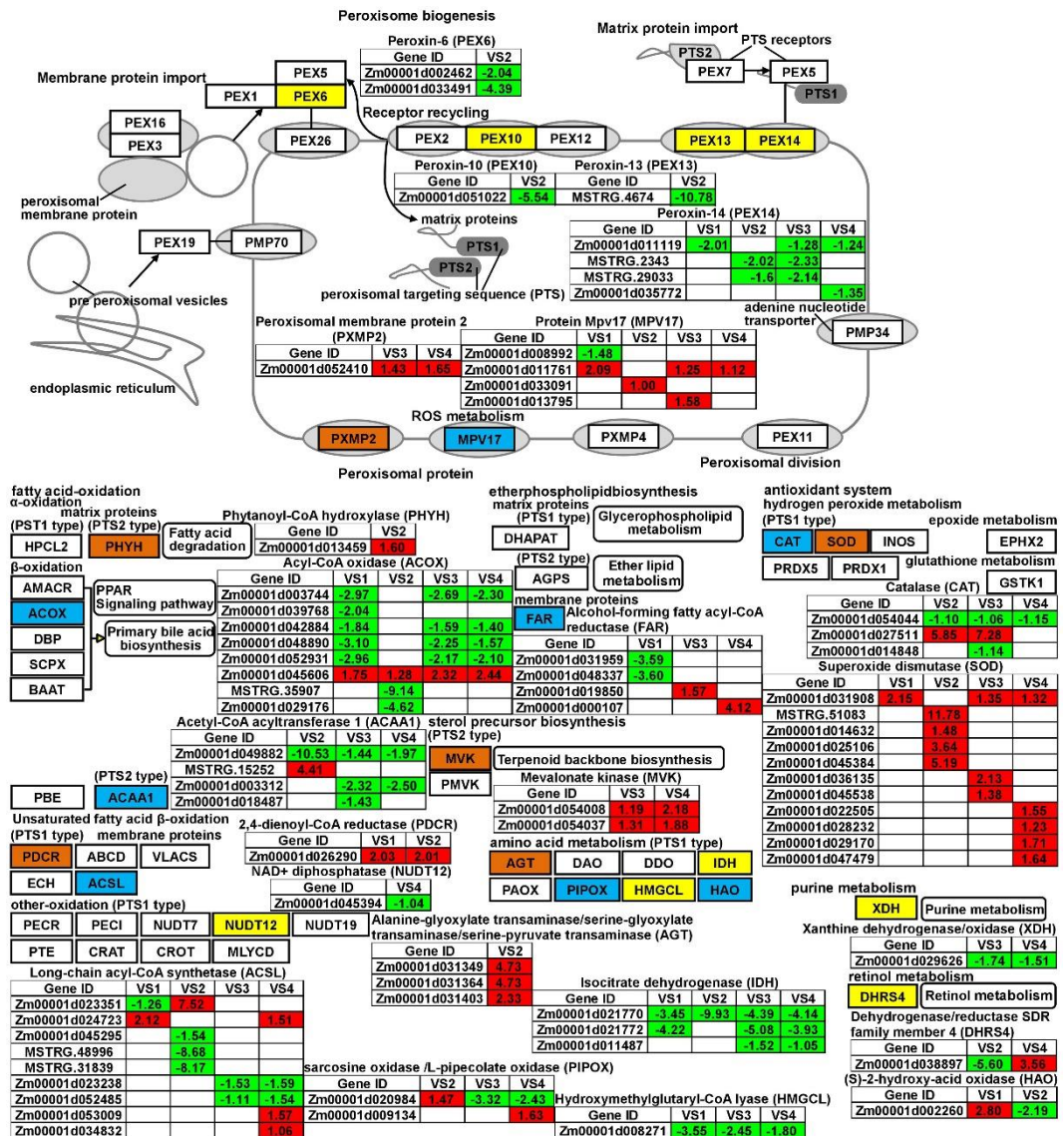


Figure S4. DEGs involved in peroxisome biogenesis that controlled lignin biosynthesis by regulating H₂O₂ level in N192 and Ji853 mesocotyls under CK, DSS, and DSS+EBR conditions.

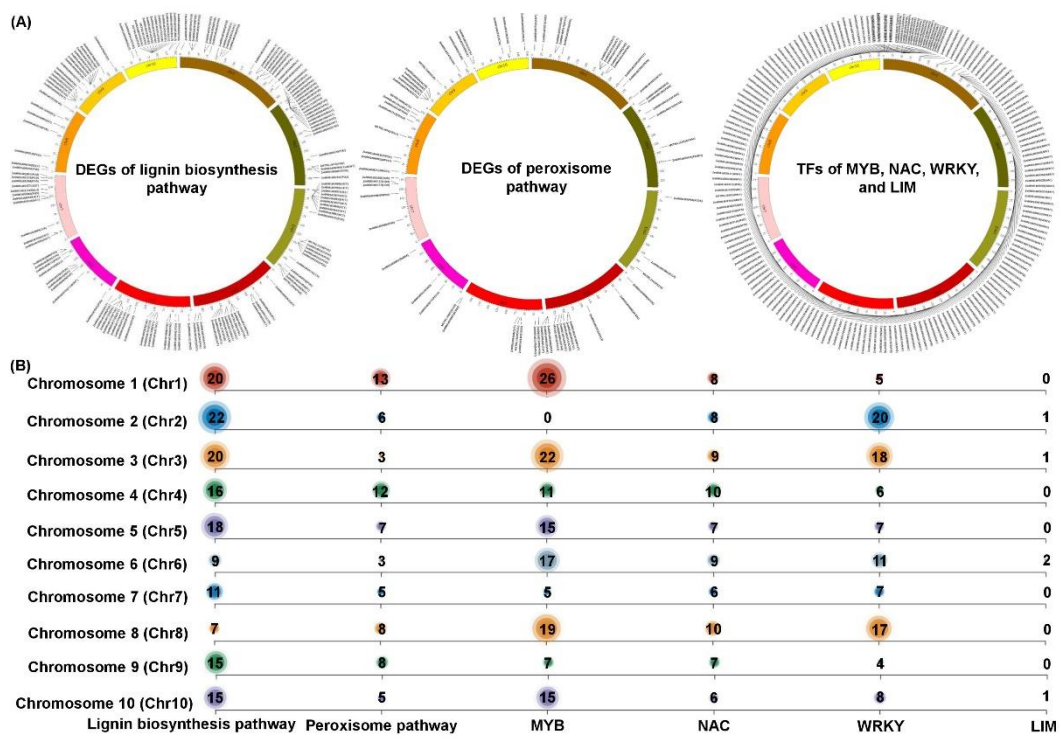


Figure S5. Genomic distributions of corresponding identified DEGs/transcription factors (TFs) on ten maize chromosomes. DEGs of lignin biosynthesis pathway, peroxisome pathway, and TFs including MYB, NAC, WRKY, and LIM distributions map (A). Bubble diagram of number for detected DEGs on each maize chromosome (B).

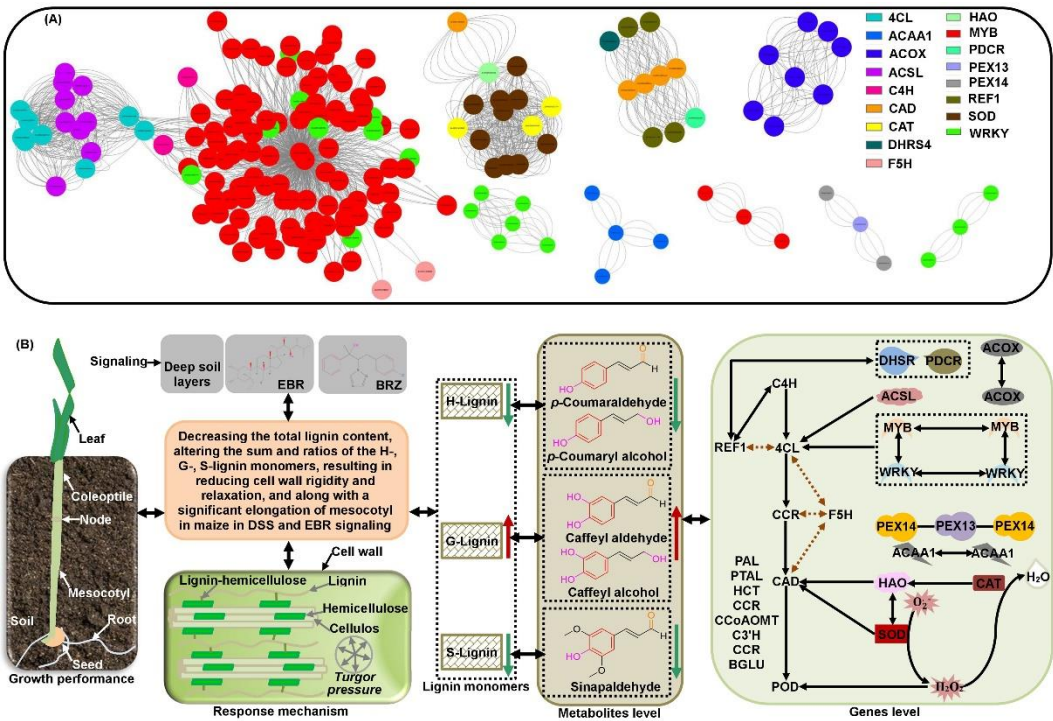


Figure S6. Interaction networks of detected DEGs and molecular network underlying the DSS and EBR signaling response of maize mesocotyl elongation. Detected DEGs of lignin biosynthesis pathway, peroxisome pathway, and corresponding TFs interactome network mapping in maize mesocotyl in DSS and EBR signaling (A). The schematic molecular model of maize mesocotyl elongation in DSS and EBR signaling (B).